Biochimica et Biophysica Acta 1853 (2015) 2144–2157

Contents lists available at ScienceDirect

Biochimica et Biophysica Acta

journal homepage: www.elsevier.com/locate/bbamcr

Extracellular S100A4 induces smooth muscle cell phenotypic transition mediated by RAGE☆

Chiraz Chaabane [a], Claus W. Heizmann [b], Marie-Luce Bochaton-Piallat [a,*]

[a] Department of Pathology and Immunology, Faculty of Medicine, University of Geneva, Geneva, Switzerland
[b] Department of Pediatrics, Division of Clinical Chemistry and Biochemistry, University of Zürich, Zürich, Switzerland

ARTICLE INFO

Article history:
Received 14 May 2014
Received in revised form 20 July 2014
Accepted 29 July 2014
Available online 7 August 2014

Keywords:
EF-hand
S100A4
RAGE
PDGF-BB
Atherosclerosis
Restenosis

ABSTRACT

We identified S100A4 as a marker of rhomboid (R) smooth muscle cells (SMCs) in vitro (the synthetic phenotype, typical of intimal SMCs) in the porcine coronary artery and of intimal SMCs in vivo in both pigs and humans. S100A4 is an intracellular Ca^{2+} signaling protein and can be secreted; it has extracellular functions via the receptor for advanced glycation end products (RAGE). Our objective was to explore the role of S100A4 in SMC phenotypic change, a phenomenon characteristic of atherosclerotic plaque formation. Transfection of a human S100A4-containing plasmid in spindle-shaped (S) SMCs (devoid of S100A4) led to approximately 10% of S100A4-overexpressing SMCs, S100A4 release, and a transition towards a R-phenotype of the whole SMC population. Furthermore treatment of S-SMCs with S100A4-rich conditioned medium collected from S100A4-transfected S-SMCs induced a transition towards a R-phenotype, which was associated with decreased SMC differentiation markers and increased proliferation and migration by activating the urokinase-type plasminogen activator (uPA), matrix metalloproteinases (MMPs) and their inhibitors (TIMPs). It yielded NF-κB activation in a RAGE-dependent manner. Blockade of extracellular S100A4 in R-SMCs with S100A4 neutralizing antibody induced a transition from R- to S-phenotype, decreased proliferative activity and upregulation of SMC differentiation markers. By contrast, silencing of S100A4 mRNA in R-SMCs did not change the level of extracellular S100A4 or SMC morphology in spite of decreased proliferative activity. Our results show that extracellular S100A4 plays a pivotal role in SMC phenotypic changes. It could be a new target to prevent SMC accumulation during atherosclerosis and restenosis. This article is part of a Special Issue entitled: 13th European Symposium on Calcium.

1. Introduction

The phenotypic heterogeneity of arterial SMCs is now well demonstrated, mainly by isolating in vitro distinct SMC subpopulations from the media in several species e.g. rat, dog, pig, calf and human [1,2]. Biological features such as high proliferative and migratory activities and poor level of differentiation are typical of the intimal SMCs. In the normal porcine coronary artery media, we isolated, in addition to the classical spindle-shaped (S) SMCs, the rhomboid (R) SMCs. R-SMCs were also recovered in higher proportion from the experimentally stent-induced intimal thickening and exhibited features compatible with their accumulation in the intima (i.e. enhanced proliferative and migratory activities and poor level of differentiation) [3]. By means of a proteomic approach, we identified S100A4 as a marker of R-SMCs in vitro and of intimal SMCs in vivo, in both pig and human arteries [4,5].

S100A4 belongs to a large family of low molecular weight Ca^{2+}-binding S100 proteins characterized by the EF-hand structural motif [6,7]. Most S100 proteins can form homo- or heterodimers as well as higher polymers [6]. Intracellular S100A4 is well established as a mediator of cancer metastasis; in humans, it is correlated with poor cancer prognosis and is used to evaluate the metastatic potential of various carcinomas [8–10]. S100A4 is synthesized and secreted from tumor and stroma cells [11,12]. It exhibits both intra- and extracellular functions related to mechanisms that could explain the contribution of S100A4 to the proliferative and metastatic potential of cancer cells. Intracellular S100A4 promotes cell proliferation via its binding and sequestration of the tumor-suppressor protein p53, abrogating the progression of the cell division cycle [8,13,14], whereas extracellular S100A4 enhances cell proliferation by interacting with epidermal growth factor receptor ligands [8,14,15]. Intracellular S100A4 inhibits phosphorylation of target proteins in a Ca^{2+} dependent manner such as non-muscle myosin heavy chain [16]. Moreover S100A4 could also interact with other cytoskeletal proteins, including actin [17] and non-muscle tropomyosin [18]. These processes could influence cell shape and motility. As an

Abbreviations: α-SMA, α-smooth muscle actin; CM, conditioned medium; MMP, matrix metalloproteinase; PDGF-BB, platelet-derived growth factor-BB; PDTC, pyrrolidine dithiocarbamate; RAGE, receptor for advanced glycation end products; R, rhomboid; SMC, smooth muscle cell; SMMHC, smooth muscle myosin heavy chain; S, spindle-shaped; TIMPs, tissue inhibitors of metalloproteinases; uPA, urokinase-type plasminogen activator

☆ This article is part of a Special Issue entitled: 13th European Symposium on Calcium.

* Corresponding author at: University of Geneva-CMU, Department of Pathology and Immunology, Rue Michel Servet-1, 1211 Geneva 4, Switzerland. Tel.: +41 22 379 5764; fax: +41 22 379 5746.
E-mail address: Marie-Luce.Piallat@unige.ch (M.-L. Bochaton-Piallat).

http://dx.doi.org/10.1016/j.bbamcr.2014.07.022
0167-4889/

extracellular protein, S100A4 through the receptor for advanced glycation end products (RAGE), a member of the superfamily of immunoglobulin molecules [6], induces migration and production of matrix metalloproteinases (MMPs) in various cells including tumor cells and endothelial cells [8,14].

Herein we investigated whether modulation of S100A4 expression and/or release induces phenotypic and biological changes in porcine coronary artery S- and R-SMC populations. By using S100A4 plasmid transfection and S100A4-rich conditioned medium (CM) treatment in S-SMCs as well as silencing S100A4 mRNA and neutralizing S100A4 antibody in R-SMCs we conclude that extracellular S100A4 is essential for the transition from S- to R-phenotype.

2. Material and methods

2.1. Cell culture and treatment

Coronary arteries of 8 month-old pigs were obtained from a nearby slaughterhouse. SMCs with different phenotypes were isolated from the porcine coronary artery media using enzymatic digestion (S-SMCs) or tissue explantation (R-SMCs, $n = 15$ for each phenotype). Endothelial cells were also isolated from porcine aorta ($n = 4$) [3]. SMCs between the 6th and 11th passages were plated at a density of 60 cells/mm^2 in 60 mm culture dishes containing Dulbecco's modified eagle medium (DMEM, Gibco-Invitrogen, Basel, Switzerland) supplemented with 10% fetal calf serum (FCS, Amimed, Bioconcept, Allschwil, Switzerland). After 24 h, S- and R-SMCs were treated with 30 ng/mL human recombinant platelet-derived growth factor-BB (PDGF-BB, Sigma, Buchs, Switzerland) for 48 h to induce phenotypic changes and/or S100A4 up-regulation [4]. To neutralize the activity of extracellular S100A4, R-SMCs were plated in DMEM plus 10% FCS containing 100 μg/mL specific rabbit polyclonal anti-human recombinant S100A4 (Thermo Scientific, Basel, Switzerland) for 96 h. This antibody does not cross-react with other S100 proteins and has been shown to markedly attenuate migratory activities in pulmonary artery SMCs [19]. Unspecific rabbit polyclonal IgGs were used as control at the same concentration. RAGE antagonistic peptide (RAP, Thermo Scientific, Basel, Switzerland) was dissolved in dimethyl sulfoxide at 40 mM and added to S-SMCs at a final concentration of 30 μM 2 h before adding conditioned medium (CM) collected from pcDNA3- or pcDNA3-S100A4 transfected S-SMCs. S-SMCs were treated with 20 μM pyrrolidine dithiocarbamate (PDTC; Sigma, Buchs, Switzerland) for 30 min to inhibit NF-κB activation before adding CM.

2.2. Small interfering RNA and plasmid transfection

Specific siRNA expression vectors homologous to the coding sequence of pig S100A4 (S100A4 siRNA) from nucleotide position 186 to 206 and pig RAGE (RAGE siRNA) from nucleotide position 469 to 487 were selected. Nonsilencing (scramble) siRNAs were used as a negative control. Human S100A4 pcDNA3 vector (pcDNA3-S100A4) and empty pcDNA3 vector (pcDNA3) as a negative control were used. Transfection of siRNA (40 nM for S100A4 and 160 nM for RAGE) and pcDNA3 (1 μg/mL) was performed on adherent SMCs using Lipofectamine 2000 (2 μL/mL, Gibco-Invitrogen) in OptiMEM (Gibco-Invitrogen). After 6 h, the medium was replaced with DMEM containing 10% FCS during 48 and 96 h for pcDNA3 vector transfection or during 48 h for siRNA transfection. The medium was not changed during the time of the experiments. Cells were fixed and processed for immunofluorescence staining or harvested for Western blotting and real-time PCR. These experiments were repeated at least 3 times for each transfection. S100A4 transfected SMC supernatants were also collected after 48 and 96 h for immunoprecipitation and competitive ELISA. Block-it Fluorescent Oligo (Gibco-Invitrogen) was used as positive control of transfection efficiency.

2.3. Conditioned medium treatment

Medium of S-SMC transfected with pcDNA3 or with pcDNA3-S100A4 for 48 h was used as source of conditioned medium (CM). S-SMCs used as target cells were plated at a density of 60 cells/mm^2 in 60 mm culture dishes for 24 h. The culture medium was replaced by the fresh CM from S-SMCs transfected with empty (pcDNA3-CM) or S100A4 (S100A4-CM) vector, for 48 and 96 h. CM-treated S-SMCs were fixed and immunostained for immunofluorescence. Protein and RNA expression was examined by Western blotting and real-time PCR, respectively.

2.4. Immunofluorescence staining

Double immunofluorescence staining was performed on adherent SMCs. Cells were fixed for 30 min in DMEM with 2% HEPES (Gibco-Invitrogen) and 1% paraformaldehyde (PFA, Fluka, Buchs, Switzerland), then rinsed in PBS and further incubated for 5 min in methanol at −20 °C. After washing in PBS, cells were double stained with mouse monoclonal IgG2a antibody recognizing α-smooth muscle actin (α-SMA, clone 1A4) [20] and a homemade mouse monoclonal IgM recognizing the C-terminal sequence of S100A4 which does not cross with other S100 proteins [4] or with rabbit polyclonal IgG specific for NF-κB (P65, Santa Cruz Biotechnology, Inc., Heidelberg, Germany) antibodies. Alternatively, cells were fixed for 30 s in ethanol at room temperature and stained with rabbit polyclonal IgG recognizing smooth muscle myosin heavy chains (SMMHCs, BT-562, Biomedical Technologies Inc., Stoughton, Mass). FITC-conjugated goat anti-mouse IgG2a, rhodamine-conjugated goat anti-mouse IgM, and FITC- or rhodamine-conjugated goat anti-rabbit IgG were used as secondary antibodies (Southern Lab, Birmingham, AL). Nuclei were stained by DAPI (Sigma). Slides were mounted in buffered polyvinyl alcohol. Images were taken by means of an Axioskop 2 microscope (Carl Zeiss, Jena, Germany) equipped with an oil plan-neofluar ×40/1.4 objective and a high sensitivity, high resolution digital color camera (Axiocam, Carl Zeiss) using the software Metafluor 4.01 (Carl Zeiss) and processed using Adobe Photoshop.

2.5. Cell proliferation

To identify replicating cells, cultured SMCs were synchronized in serum-free medium overnight [21], incubated with 5-bromo-2′-deoxyuridine (BrdU, 10^{-5} M, Sigma) for 18 h at 37 °C and then fixed for 5 min in methanol at −20 °C. After washing in PBS they were incubated for 20 min in 1 M HCl followed by 0.1 M Borax, pH 8.5 for 5 min. The incorporated BrdU was detected immunohistochemically using a mouse monoclonal BrdU antibody (Dako, Copenhagen, Denmark). Alexa 488-conjugated goat anti-mouse IgG (Molecular Probes, Eugene, OR) was used as secondary antibody. Nuclei were stained by DAPI. Slides were mounted in buffered polyvinyl alcohol. The percentage of BrdU-positive cells was calculated using MetaMorph 6.0 image analysis system (Universal Imaging Corporation, Biocompare, San Francisco, CA).

For evaluation of proliferation, cells were trypsinized and counted using a hemocytometer. The results were calculated as the ratio of counted to seeded cells, and then normalized as the percentage of control condition. Cells were further extracted for Western blotting.

2.6. Cell migration

S-SMCs were seeded onto matrigel-coated 96-well plates (BD Biosciences, Basel, Switzerland) and grown to confluence. Confluent cell monolayers were wounded with a pipette tip and the culture medium was replaced by the CM from S-SMCs transfected with empty (pcDNA3-CM) or S100A4 (S100A4-CM) vector for 24 h at 37 °C. The wounded areas were monitored using an ImageXpress automated

microscope equipped with a 4 objective (Molecular Devices, Sunnyvale, CA, USA). The area of cell migration was calculated using the MetaMorph 6.0 software (Molecular Devices). The results were calculated as the ratio of the area filled by migrated cells at 24 h to the wounded area at 0 h. Cell migration assays for each sample were performed in triplicate, and 3 independent experiments were carried out for each experimental condition.

2.7. Protein extraction, electrophoresis, and Western blotting

SMCs were trypsinized and proteins were extracted as previously described [4]. Protein concentration was determined according to Bradford [22]. Proteins were separated by SDS-PAGE on 4–12% mini gels (Bio-Rad, Basel, Switzerland) and stained with Coomassie brilliant blue (R250, Fluka). For Western blotting 1 μg of protein for α-SMA or 12 μg of proteins for SMMHCs and phospho-NF-κB was electrophoresed and transferred to a nitrocellulose membrane (Protran® 0.2 μm; Schleicher and Schuell, Dassel, Germany). Twelve micrograms of proteins for S100A4 was electrophoresed and transferred to a PVDF membrane (0.45 μm, Immobilon™-P, Millipore Corporation, Bedford, MA) [4]. For α-SMA detection, proteins were loaded at 1 μg because of the high level of α-SMA expression in SMCs. Membranes were incubated with anti-α-SMA, anti-S100A4, anti-SMMHCs or rabbit polyclonal IgG specific for phospho-NF-κB (Ser536, Cell Signaling Technology, Boston, MA). Mouse monoclonal IgG1 specific for vimentin and rabbit polyclonal IgG specific for glyceraldehyde 3-phosphate dehydrogenase (GAPDH) were used as housekeeping proteins. Horseradish peroxidase-conjugated goat anti-mouse IgG or IgM and goat anti-rabbit IgG were used as secondary antibodies. Enhanced chemiluminescence was used for detection (Amersham, Buckinghamshire, United Kingdom). Signals were digitized by means of Epson perfection 4990 photo scanner and analyzed using MetaMorph 6.0 image analysis system (Universal Imaging Corporation).

2.8. Immunoprecipitation and enzyme-linked immunosorbent assay (ELISA)

Supernatants from SMCs treated without or with PDGF-BB as well as transfected with pcDNA3- or pcDNA3-S100A4, and scramble or S100A4 siRNA were collected 48 and 96 h after plating for immunoprecipitation and/or competitive ELISA. Cultured SMC supernatants were transferred to microcentrifuge tubes. Protease activity was blocked by adding protease inhibitors prior to centrifugation. For immunoprecipitation, protein A Sepharose beads (Pharmacia) were incubated with rabbit polyclonal anti-human S100A4 (A5114, Dako, this antibody does not cross with other S100 proteins) or anti-actin (Rb, A5060 Sigma) for 2 h by rotation on a wheel at room temperature. Then supernatants of each sample were incubated with beads coupled to antibodies by rotation overnight at 4 °C. The complex beads–antibodies–proteins was centrifuged, washed with 50 mM TRIS pH 7.5, extracted by adding lysis buffer and boiled for 5 min at 95 °C. Twenty microliters of each sample was loaded on a 10% SDS-PAGE mini gel prior to transfer to nitrocellulose or PVDF membranes and incubated with primary and secondary antibodies as described above.

For competitive ELISA, mouse monoclonal S100A4 IgM and SMC supernatants were mixed for 1 h at room temperature and then incubated overnight at 4 °C in a 96 well-plate coated with the C-terminal 16 amino acids of S100A4 bound to BSA (20 ng/mL in 50 mM sodium bicarbonate, pH 8). Incubation with alkaline phosphatase-conjugated goat anti-mouse IgM (Southern Biotech) diluted in DMEM containing 10% FCS was performed 1 h at 37 °C. The substrate solution (p-nitrophenylphosphate; S0942, Sigma) was added and the enzymatic reaction produced a soluble yellow product measured at 405 nm. The standard curve was performed by incubating the mouse monoclonal anti-S100A4 with increasing concentrations of S100A4 peptide instead of SMC supernatants.

2.9. RNA extraction, reverse-transcription and real-time quantitative PCR

Total RNA was extracted from SMCs treated without or with PDGF-BB or CM and from endothelial cells with TRIzol reagent (Gibco-Invitrogen) and processed for reverse transcription and real-time SYBR Green fluorescent PCR. The cDNA was synthesized from total RNA with random hexamers and TAKARA Reverse Transcription (Gibco-Invitrogen). Reverse transcription was performed at 37 °C for 15 min and then at 85 °C for 5 s. The forward and reverse primers (Sigma, Buchs, Switzerland) are listed in Table 1. Real time SYBR Green fluorescent PCR was performed in an iCycler iQ® Real-Time PCR Detection System (Bio-Rad) in a final volume of 10 μL comprising 5 μL of cDNA. Each couple of primers was used at a final concentration of 0.86 μM. Denaturation was performed for 10 min at 95 °C and then DNA was amplified for 40 cycles of 15 s at 95 °C, 45 s at 60 °C and 5 min at 72 °C followed by 70 cycles of 10 s from 60 to 95 °C (+0.5 °C/cycle) for the dissociation curve. Amplifications were repeated in triplicate. Results were normalized to amplified GAPDH transcripts in the same samples and were expressed as S100A4 or RAGE mRNA quantity in arbitrary units.

2.10. Statistical analysis

Results are shown as mean ± SEM. Comparisons between treated and control groups were analyzed by the Student *t*-test. Differences were considered statistically significant at values of $P < 0.05$.

3. Result

3.1. S100A4 is expressed and released by R-SMCs

We confirmed that S100A4 mRNA as well as protein were predominantly expressed in R-SMCs when compared with S-SMCs [4] (Fig. 1A and B). S100A4 can be released from cells into the extracellular space. By means of immunoprecipitation, we detected S100A4 in R-SMC but not in S-SMC supernatants (Fig. 1C). This was quantified by a competitive ELISA where the level of extracellular S100A4 was faint in S-SMC ($0.12 \pm 0.02 \times 10^{-3}$ pM/cell) and high in R-SMC ($0.40 \pm 0.08 \times 10^{-3}$ pM/cell, $P < 0.05$; Fig. 1D) supernatants. S100A4 was not released by dead SMCs as demonstrated below.

We reported that S-SMCs shift towards a R-phenotype when cells were treated with PDGF-BB [3]. When PDGF-BB was used at 30 ng/mL, the transition from S- to R-phenotype was observed as early as 48 h; this was accompanied by an upregulation of S100A4 mRNA (Fig. 1A) and protein (Fig. 1B); but no change in the release of S100A4 (Fig. 1C and D) was observed.

Quite in contrast, treatment of R-SMCs with PDGF-BB did increase neither S100A4 mRNA (Fig. 1A) nor protein levels (Fig. 1B) probably due to the high concentration of endogenous S100A4 already present in untreated R-SMCs. However, incubation of R-SMCs with PDGF-BB markedly elevated S100A4 release in the R-SMC supernatant when compared to untreated cells as shown by means of immunoprecipitation (Fig. 1C) and ELISA (0.77 ± 0.14 vs $0.40 \pm 0.08 \times 10^{-3}$ pM/cell, respectively, $P < 0.05$; Fig. 1D). Therefore R-SMCs express and release S100A4 into the extracellular space, which is increased by PDGF-BB.

3.2. Overexpression of S100A4 in S-SMCs induces a transition from S- to R-phenotype

S100A4 overexpression was performed in S-SMCs, in which S100A4 was below detection level. The percentage of S100A4-overexpressing S-SMCs after transfection with the human S100A4 vector (pcDNA3-S100A4) represented approximately 10% (Fig. 2A, f). This percentage was similar to the transfection efficiency evaluated by transfecting the empty vector coupled to GFP (data not shown). S-SMCs transfected with pcDNA3-S100A4 acquired a R-phenotype as early as 48 h after

Table 1
Oligonucleotide sequence of porcine genes for quantitative real-time-PCR.

	Forward	Nucleotide position	Reverse	Nucleotide position
S100A4	5′-GCGATGCAGGACAGGAAGAC-3′	63–82	5′-GGCCCTCGATGTGATGGTGT-3′	271–290
RAGE	5′-GTAGCTTCAGCCCGAGCTTT-3′	700–719	5′-CACCAACTGGACTTCCTCCA-3′	780–899
PDGF-BB	5′-CGTCTGTCTCGATGCCTGATT-3′	204–223	5′-GTCAGTAGAGGAAGAGAGCGATG-3′	353–372
SM22-α	5′-GGCTGAAGAATGGCGTGAT-3′	164–183	5′-CTGCCATGTCTTTGCCTTCA-3′	354–373
c-myc	5′-GCTGGATTTCCTTCGGATAG-3′	591–610	5′-TTGGTGAAGCTGACGTTGAG-3′	636–657
SMMHCs	5′-AGGACCAGTCCATTTTGTGC-3′	674–693	5′-CCTGGTCCTTCTTGCTCTTG-3′	770–789
SMA	5′-GGGAATGGGACAAAAAGACA-3′	102–121	5′-ATGTCGTCCCAGTTGGTGAT-3′	192–211
Smoothelin	5′-GGAGAACTGGCTGCACTCTC-3′	404–423	5′-CAGCTCCTCCACATCACTCA-3′	484–503
MMP-1	5′-TCTCACCCTTGACCTTCACC	622–641	5′-TTCCTCCAGGTCCATCAAAG-3′	709–728
MMP-2	5′-CTGGTGCTGCCACACTTTAG-3′	2328–2347	5′- GGGTGCTGTAAGCCACAGA-3′	2369–2388
MMP-3	5′-ACCCTGGGTTTTCCTTCAAC-3′	575–594	5′-TGGCTCCATGGATTGTCTCT-3′	688–707
MMP-9	5′-ACGCATTGGGCTTAGATCAC-3′	1211–1230	5′-AGGTTTAGGGCGAGAACCAT-3′	1324–1343
MMP-14	5′-TGCAGCAGTATGGCTACCTG-3′	110–130	5′-CTCGCAGACCGTAGAACCTC-3′	200–220
uPA	5′-TCTTGAGAGAGCTTGGCCAA-3′	557–576	5′-TGCAAACACACACACGCATA-3′	684–703
TIMP-1	5′-GGTCATCAGGGCCAAGTTTG-3′	132–151	5′-GGGGTGTAGATGAACCGGAT-3′	253–272
TIMP-3	5′-CTTCACCAAGATGCCCCATG-3	526–545	5′-CTTGCCATCATAGACACGGC-3′	627–646
GAPDH	5′-TCTCATGGTTCACGCCCATC-3′	241–260	5′-TGGAGTCCACTGGTGTCTTC-3′	350–369

transfection. This morphological change was sustained up to 96 h (Fig. 2A, e). By contrast, S-SMCs transfected with the pcDNA3 alone (Fig. 2A, b) maintained their S-phenotype at both time points (Fig. 2A, a). S100A4 overexpression resulted in a disorganization of α-SMA-positive stress fibers (Fig. 2A, g) and a quasi-disappearance of SMMHCs (Fig. 2A, h) compared with pcDNA3-transfected cells (Fig. 2A, c and d).

Immunoblots confirmed that S100A4 was upregulated 48 and 96 h after transfection (305 ± 44%, $P < 0.01$ and 718 ± 123%, $P < 0.001$, respectively Fig. 2B). S100A4 overexpression was associated with a significant reduction of α-SMA expression (62 ± 8%, $P < 0.01$ at 48 h and 42 ± 3%, $P < 0.001$ at 96 h), and to a greater extent, of SMMHC expression (15 ± 5%, $P < 0.001$ at 48 h and 18 ± 4%, $P < 0.001$ at 96 h; Fig. 2B). In addition, at 96 h pcDNA3-S100A4-transfected cells exhibited enhanced BrdU incorporation compared with pcDNA3-transfected cells (65 ± 2% vs 53 ± 3%, $P < 0.01$, respectively; Fig. 2C) indicating that S100A4 overexpression is accompanied by increased SMC proliferation.

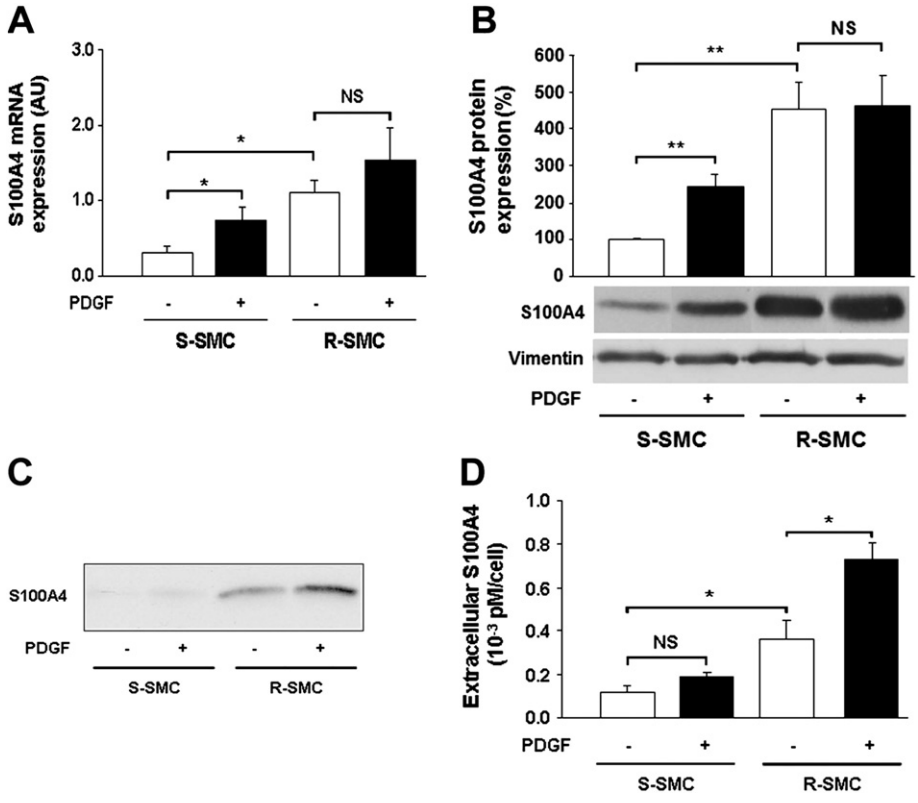

Fig. 1. Expression and release of S100A4 by S- and R-SMCs in the presence and absence of PDGF-BB. A, Bar graph showing S100A4 mRNA quantification by real-time PCR normalized to GAPDH mRNA expression in S- and R-SMCs treated without (open bars) or with (filled bars) PDGF-BB (30 ng/mL for 48 h, n = 6 for each phenotype). B, Bar graph and representative immunoblot showing S100A4 expression normalized to vimentin content in S- and R-SMCs treated without (open bars) or with (filled bars) PDGF-BB (n = 5 for each phenotype). C, Representative immunoblot for S100A4 immunoprecipitation in S- and R-SMC supernatants treated without or with PDGF-BB (n = 4 for each phenotype). D, Bar graph showing extracellular S100A4 content detected by competitive ELISA in S- and R-SMC supernatants treated without (open bars) or with (filled bars) PDGF-BB (n = 6 for each phenotype). ** = $P < 0.01$; * = $P < 0.05$; NS, not significant; AU, arbitrary units.

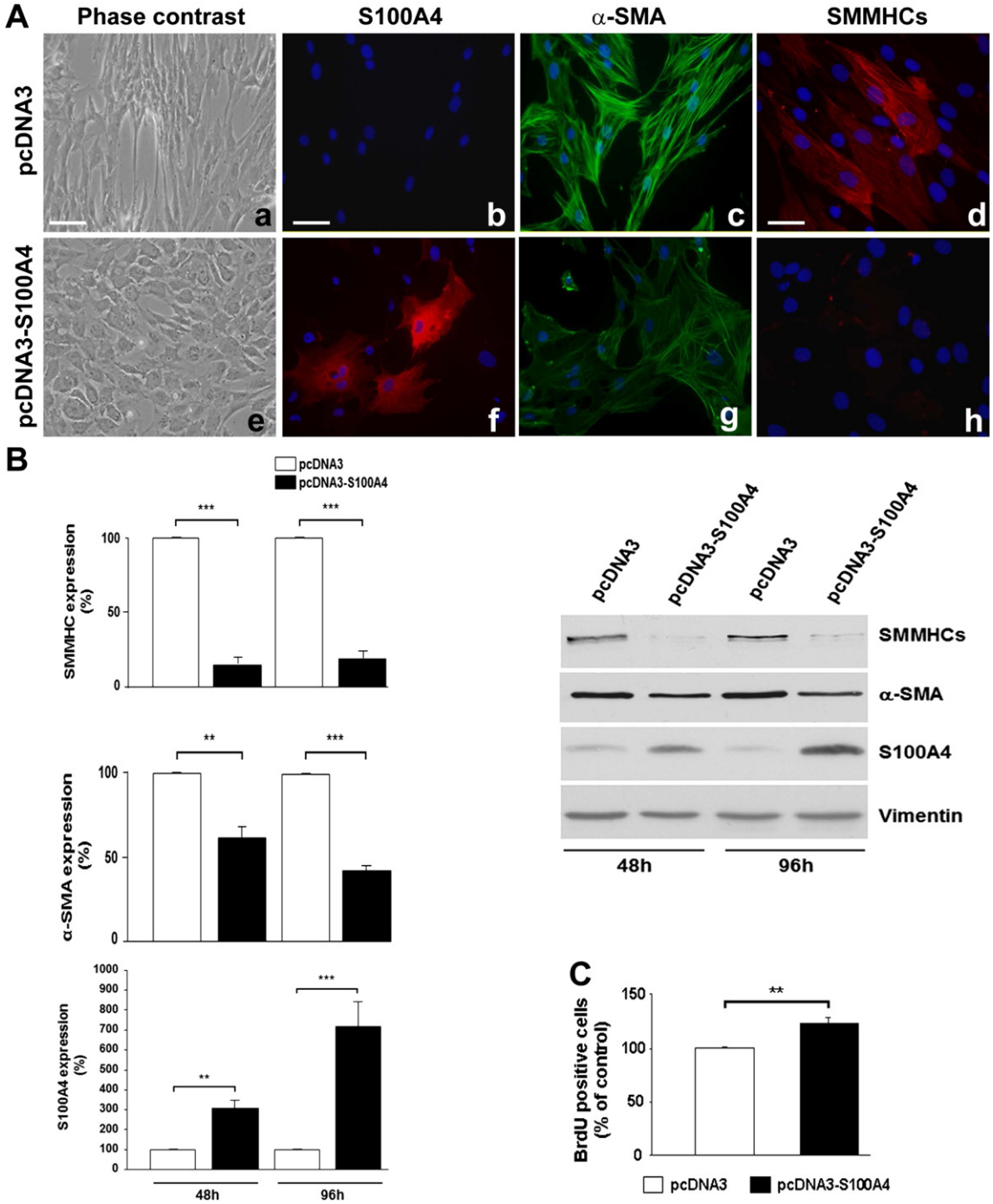

Fig. 2. Effects of S100A4 overexpression on S-SMC phenotype. A, Phase-contrast photomicrographs (a and e) and double immunofluorescence staining showing S100A4 (b and f), α-SMA (c and g) and SMMHC (d and h) expression in S-SMCs 96 h after transfection with pcDNA3 (a–d) or pcDNA3-S100A4 (e–h) vectors (n = 6). Nuclei are stained in blue by DAPI. In (a and e), bar = 75 μm; in (b, c, f and g), bar = 25 μm; in (d and h), bar = 10 μm. B, Bar graph and representative immunoblots showing S100A4, α-SMA and SMMHC expression normalized to vimentin content in S-SMCs 48 and 96 h after transfection with pcDNA3 (open bars) or pcDNA3-S100A4 (filled bars) vectors (n = 4). C, Bar graph showing the percentage of BrdU-positive cells in S-SMCs 96 h after transfection with pcDNA3 (open bars) and pcDNA3-S100A4 (filled bars) vectors (n = 3). *** = $P < 0.001$; ** = $P < 0.01$.

3.3. Overexpression of S100A4 in S-SMCs induces its release in the cell supernatant

Because 10% of S100A4-overexpressing S-SMCs led to the S- to R-phenotypic transition of the whole SMC population, we assumed that S100A4 was released into the cell supernatant affecting most of the neighboring cells. We performed immunoprecipitation of the cell supernatant, and demonstrated that S100A4 was released from the pcDNA3-S100A4- but not from the pcDNA3-transfected cells (Fig. 3A). To rule out the possibility that the presence of S100A4 in the supernatant did not leak out of dead SMCs after transfection, we measured in the supernatant of transfected cells by means of immunoprecipitation the presence of actin, a cytoskeletal protein known to be expressed exclusively intracellularly. As expected, actin was absent in the cell supernatant of pcDNA3-S100A4- and pcDNA3-transfected cells at both time points (Fig. 3A). To verify that our assay was sensitive enough i.e. actin can be detected in the cell supernatant, we lysed SMCs by means of sonication to release intracellular proteins into the supernatant. In this

condition, both actin and S100A4 were detected in the cell supernatants (Fig. 3B). Therefore, S100A4 was released by pcDNA3-S100A4-transfected S-SMCs and did not leak out of dead SMCs. Competitive ELISA confirmed that the extracellular S100A4 level was higher in pcDNA3-S100A4- than in pcDNA3-transfected S-SMCs at 48 h (1.06 ± 0.14 vs $0.18 \pm 0.03 \times 10^{-3}$ pM/cell, respectively, $P < 0.001$) and 96 h (0.97 ± 0.26 vs $0.10 \pm 0.02 \times 10^{-3}$ pM/cell, respectively, $P < 0.001$; Fig. 3C).

3.4. Extracellular S100A4-rich conditioned medium (CM) induces a transition from S- to R-phenotype

To further investigate whether extracellular S100A4 was responsible for the S- to R-phenotypic change, we used pcDNA3-S100A4 transfected S-SMC supernatant (48 h post-transfection) as source of CM and S-SMCs as target cells. pcDNA3-transfected S-SMC supernatant was used as control. In the presence of extracellular S100A4-rich CM, S-SMCs acquired a R-phenotype as early as 48 h; this change was maintained up to 96 h (Fig. 4A, a and e). However an exposure of S100A4-rich CM up to 96 h was required to observe an upregulation of intracellular S100A4 expression (Fig. 4A, f) and a downregulation of α-SMA (Fig. 4A, g) and SMMHC expression (Fig. 4A, h) compared with control conditions (Fig. 4A, b–d).

Immunoblots confirmed that S100A4-rich CM treatment for 96 h resulted in increased S100A4 ($392 \pm 61\%$, $P < 0.001$) and decreased α-SMA and SMMHC ($20 \pm 4\%$, $P < 0.001$ and $11 \pm 4\%$, $P < 0.001$, respectively; Fig. 4B) contents compared with control conditions. S100A4 mRNA content was as well increased after S100A4-rich CM treatment compared with control conditions as later as 96 h ($600 \pm 1\%$, $P < 0.001$, $n = 3$).

To ascertain that S100A4-rich CM treated S-SMCs exhibited a phenotype similar to the one of native R-SMCs, we analyzed by real-time PCR the expression of genes typically involved in SMC differentiation (SM22-α, α-SMA, SMMHC and smoothelin) [1,2,23] and dedifferentiation (S100A4, PDGF-BB and c-myc) [2–4]. SMC differentiation markers were downregulated and SMC dedifferentiation markers were upregulated in S100A4-rich CM treated S-SMCs and native R-SMCs when compared with pcDNA3-CM treated S-SMCs and native S-SMCs, respectively (Table 2). When these results were normalized to their respective controls, the level of S100A4 and PDGF-BB mRNA was markedly higher in native R-SMCs compared with S100A4-rich CM treated S-SMCs (Fig. 5A). Therefore, the R-phenotype observed after treatment with S100A4-rich CM exhibits mRNA profile close to the one of native R-SMCs with respect to SMC differentiation/dedifferentiation markers.

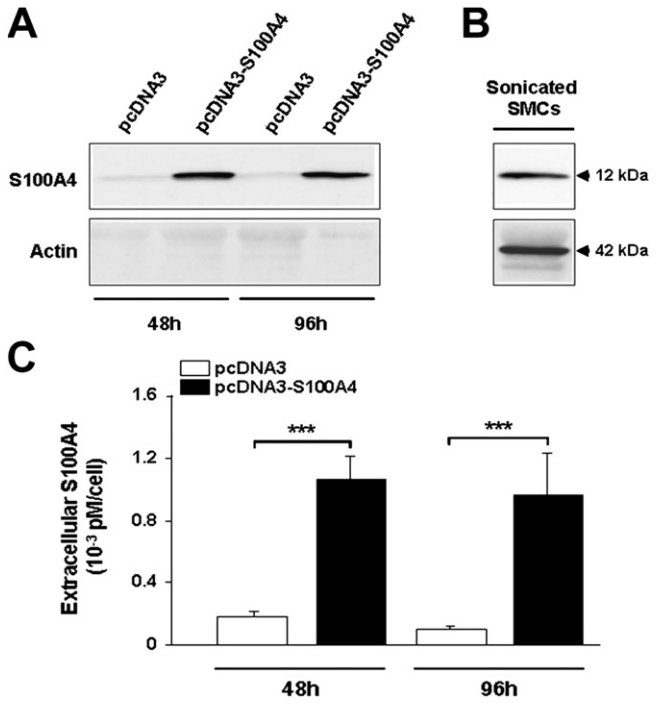

Fig. 3. Effects of S100A4 overexpression in S-SMCs on S100A4 release. A, Representative immunoblots for S100A4 and actin immunoprecipitation in S-SMC supernatants 48 and 96 h after transfection with pcDNA3 or pcDNA3-S100A4 vectors (n = 4). B, Representative immunoblots for S100A4 and actin immunoprecipitation in lysed SMC supernatants i.e. dead cells. C, Bar graph showing extracellular S100A4 content detected by competitive ELISA in S-SMC supernatants after transfection with pcDNA3 (open bars) and pcDNA3-S100A4 (filled bars) vectors (n = 4). *** = $P < 0.001$.

3.5. Extracellular S100A4-rich CM enhances SMC proliferative, migratory and proteolytic activities

Cell proliferation was enhanced in S-SMCs treated with S100A4-rich CM as later as 96 h after treatment ($150 \pm 8\%$, $P < 0.01$; Fig. 4C) compared with control conditions. Cell migration assays showed that S-SMCs treated with S100A4-rich CM for 24 h exhibited enhanced migratory activity (Fig. 4D, b and d) compared with control conditions (Fig. 4D, a and c; ratio of filled area at 24 h/wounded area at 0 h: $193 \pm 56\%$ vs $2 \pm 0.29\%$, $P < 0.001$, respectively; Fig. 4D). Over 24 h of treatment S-SMC replication was hence negligible. We further examined mRNA expression of MMPs, tissue inhibitors of metalloproteinases (TIMPs) and urokinase-type plasminogen activator (uPA) by real-time PCR (Table 3 and Fig. 5B). When S-SMCs were treated with S100A4-rich CM, MMP-1, -2, -3, and -9 and uPA were increased and MMP-14 was decreased compared with pcDNA3-CM treated S-SMCs. By contrast, when native R-SMCs were compared with S-SMCs only MMP-2 and uPA were increased whereas the other MMPs were either not modified (MMP-9 and -14) or slightly decreased (MMP-1 and -3). In S100A4-rich CM treated S-SMCs, TIMP-1 was increased while TIMP-3 was decreased compared with control conditions. The opposite result was observed in native R-SMCs versus S-SMCs. Therefore, the R-phenotype observed after treatment with S100A4-rich CM exhibits mRNA profile distinct from the one of native R-SMCs as far as proteolytic enzymes and their inhibitors are concerned.

3.6. Neutralization of extracellular S100A4 induces a transition from R- to S-phenotype

We explored the role of extracellular S100A4 activity in R-SMCs. When treated with rabbit polyclonal neutralizing S100A4 antibody [19] for 96 h, R-SMCs modulated towards a S-phenotype (Fig. 6A, e). Unspecific rabbit polyclonal antibodies, used as control, had no effect (Fig. 6A, a). Double immunofluorescence staining showed that intracellular S100A4 (Fig. 6A, f) expression was strongly decreased whereas α-SMA (Fig. 6A, g) and SMMHC (Fig. 6A, h) expression was increased after treatment with neutralizing anti-S100A4 compared with control conditions (Fig. 6A, b–d). Immunoblots confirmed that neutralization of extracellular S100A4 resulted in decreased S100A4 content and increased α-SMA and SMMHC contents compared with control condition (Fig. 6B). Neutralization of extracellular S100A4 activity markedly reduced R-SMC proliferation compared with control conditions ($68 \pm 4\%$, $P < 0.001$; Fig. 6C). Therefore blockade of extracellular S100A4 activity reverses the phenotype from R- to S-phenotype, which is associated with decreased intracellular S100A4 expression and proliferative activity and increased SMC differentiation marker expression.

3.7. Downregulation of intracellular S100A4 in R-SMCs and PDGF-BB-treated S-SMCs reduces cell proliferation

Downregulation of endogenous S100A4 in R-SMCs, in which S100A4 is highly expressed, was performed by using S100A4-specific siRNA [4]. The number of S100A4-positive-SMCs was substantially decreased after

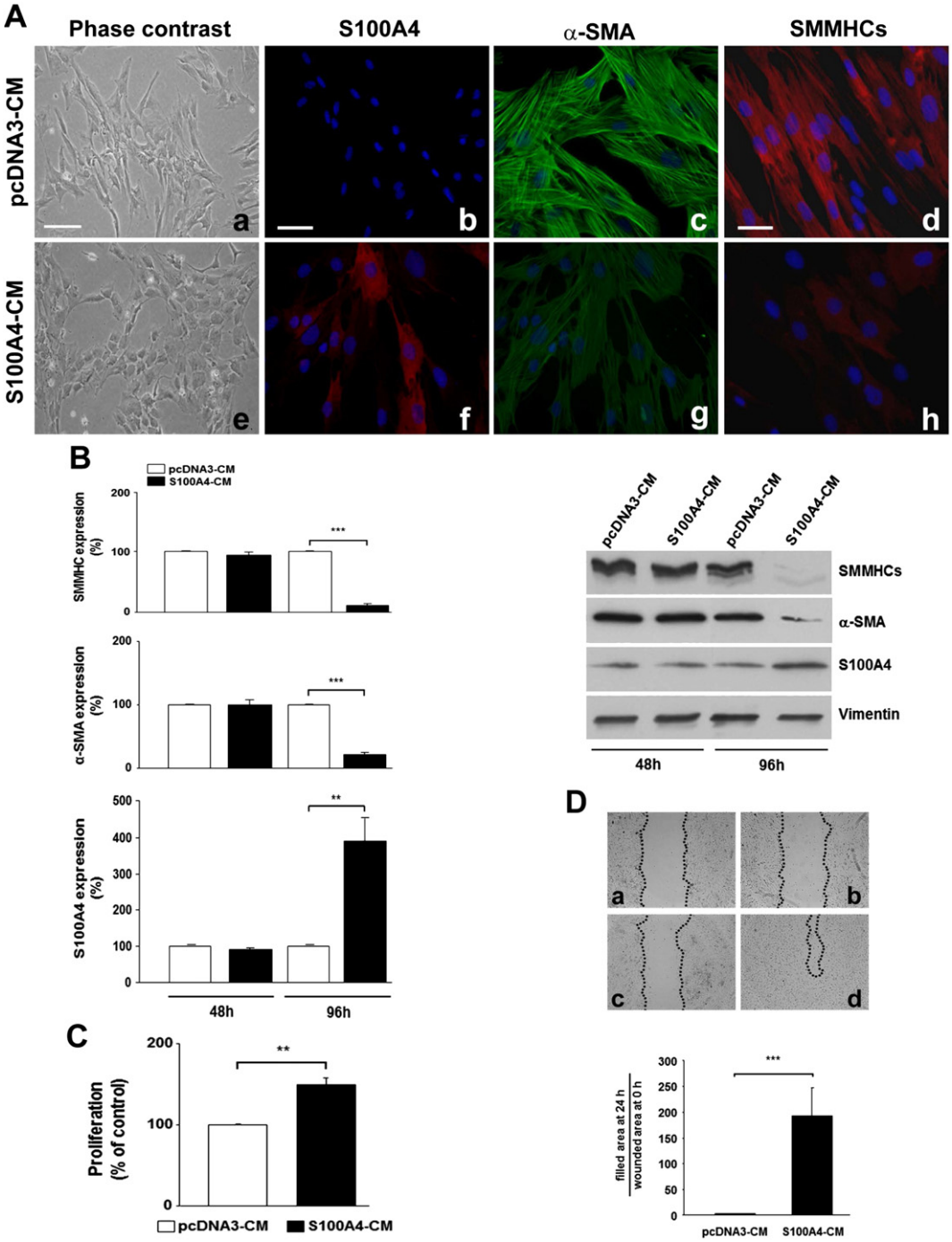

Fig. 4. Effect of extracellular S100A4-rich CM on S-SMC phenotype. A, Phase-contrast photomicrographs (a and e) and double immunofluorescence staining showing S100A4 (b and f), α-SMA (c and g) and SMMHC (d and h) expression in S-SMCs treated for 96 h with CM collected from pcDNA3 (a–d) or pcDNA3-S100A4 (e–h) vector transfected S-SMCs (48 h post-transfection, n = 5). In (a and e), bar = 75 μm; in (b, c, f and g), bar = 25 μm; in (d and h), bar = 10 μm. B, Bar graph and representative immunoblots showing S100A4, α-SMA and SMMHC expression normalized to vimentin content in S-SMCs treated for 48 and 96 h with CM collected from pcDNA3 (open bars) or pcDNA3-S100A4 (filled bars) vector transfected S-SMCs (48 h post-transfection, n = 4). C, Bar graph showing S-SMC proliferation treated for 96 h with CM collected from pcDNA3 (open bar) or pcDNA3-S100A4 (filled bar) vector transfected S-SMCs (48 h post-transfection, n = 4). *** = $P < 0.001$; ** = $P < 0.01$. D, Cell migration assay showing migratory activity of S-SMCs treated with CM collected from pcDNA3 (a and c) or pcDNA3-S100A4 (b and d) vector transfected S-SMCs (48 h post-transfection, n = 8) at 0 (a and b) and 24 (c and d) h. Bar graph showing the ratio of filled area at 24 h/wounded area at 0 h in S-SMCs treated for 24 h with CM collected from pcDNA3 (open bars) or pcDNA3-S100A4 (filled bars) vector transfected S-SMCs. *** = $P < 0.001$.

transfection of S100A4-specific siRNA compared with scramble siRNA (Fig. 7A, b and e). Immunoblots confirmed that S100A4-specific siRNA treatment decreased the S100A4 content (46 ± 13%, $P < 0.001$, Fig. 7B). Although no phenotype reverse was observed (Fig. 7A, a and d), S100A4 silencing was associated with a slight increase of α-SMA expression as shown by immunofluorescence staining (Fig. 7A, c and f) and of α-SMA content (111 ± 1%, $P < 0.05$; Fig. 7B) as shown by Western blotting. Nevertheless, depletion of S100A4 for 48 h did not modify the level of extracellular S100A4 present in the supernatant compared with control (1.06 ± 0.01 vs 0.92 ± 0.2 × 10^{-3} pM/cell, respectively; Fig. 7C). However, silencing of S100A4 reduced R-SMC proliferation compared with control condition (Fig. 7D). These data suggest that

Table 2
Expression of SMC differentiation/dedifferentiation mRNAs in S100A4-rich CM treated S-SMCs and native R-SMCs compared with their respective controls.

	S-SMCs treated with			Native		
	PcDNA3-CM	S100A4-CM	*P*	S-SMC	R-SMC	*P*
Upregulated mRNA						
S100A4	2.87 ± 0.01	14.63 ± 0.01	$P < 0.001$	5.81 ± 0.01	94.77 ± 0.03	$P < 0.001$
PDGF-BB	6.00 ± 0.01	20.38 ± 0.01	$P < 0.001$	10.82 ± 0.01	60.69 ± 0.16	$P < 0.05$
c-myc	45.11 ± 0.04	67.39 ± 0.02	$P < 0.01$	76.18 ± 0.06	97.76 ± 0.25	NS
Downregulated mRNA						
SM22-α	176.21 ± 0.10	43.71 ± 0.02	$P < 0.001$	101.83 ± 0.20	34.69 ± 0.06	$P < 0.01$
α-SMA	208.51 ± 0.04	18.02 ± 0.07	$P < 0.001$	111.62 ± 0.07	29.32 ± 0.14	$P < 0.01$
SMMHC	142.84 ± 0.18	65.70 ± 0.01	$P < 0.01$	134.78 ± 0.22	88.89 ± 0.06	$P < 0.05$
Smoothelin	158.93 ± 0.29	39.58 ± 0.08	$P < 0.01$	102.34 ± 0.24	27.99 ± 0.10	$P < 0.05$

mRNA expression is normalized to GAPDH mRNA expression (%).

intracellular S100A4 is involved in SMC proliferation and that the presence of extracellular S100A4 in the supernatant maintains the R-phenotype.

In S-SMCs, the morphological change observed in PDGF-BB-induced S- to R-phenotypic transition (see Section 3.1) was not reversed by treatment with silencing S100A4 (Fig. 8A, a and d). However, the PDGF-BB-induced S100A4 upregulation and α-SMA downregulation (Fig. 8A, c and f) were abolished by silencing S100A4. Immunoblots confirmed that downregulation of S100A4 content (19 ± 10%, $P < 0.001$; Fig. 8B) noticeably prevented the PDGF-BB-induced α-SMA downregulation (147 ± 7%, $P < 0.001$; Fig. 8B) and SMC proliferative activity (69 ± 5%, $P < 0.01$; Fig. 8C). Taken together, our results indicate that downregulation of intracellular S100A4 in R-SMCs or PDGF-BB-treated S-SMCs (i.e. promoting S- to R-phenotypic transition) does not affect SMC morphology even if it has a partial effect on SMC differentiation marker expression and proliferative activity.

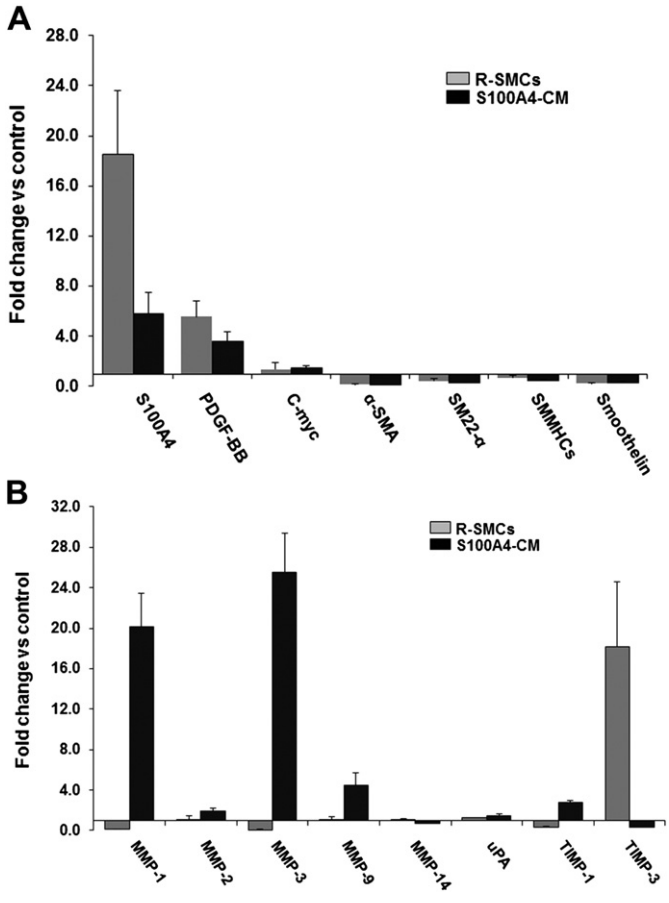

Fig. 5. Comparison of SMC dedifferentiation/differentiation marker (A), MMP and TIMP (B) expression in native R-SMCs and S100A4-rich CM treated S-SMCs. In A and B, bar graphs show mRNA fold change in native R-SMCs and S100A4-rich CM treated S-SMCs normalized to their respective controls. Data corresponds to the mean values described in Tables 2 and 3.

3.8. Extracellular S100A4-rich CM induces RAGE and NF-κB activation

S100A4 interacts with RAGE in vitro as demonstrated by surface plasmon resonance study [24] but this interaction appears to be more complex in vivo [8,9]. After treatment of S-SMCs with S100A4-rich CM for 4 h, RAGE mRNA was increased compared with control conditions (0.64 ± 0.04% vs 0.24 ± 0.03%, $P < 0.01$; Fig. 9A). Porcine aortic endothelial cells were used as a positive control (1.71 ± 0.37%). Several studies demonstrate a correlation between RAGE expression and NF-κB pathway activation [11,12]. In the presence of extracellular S100A4-rich CM for 1 h, translocation of NF-κB from the cytosol to the nucleus (Fig. 9B) and increased phosphorylation of NF-κB (Fig. 9D) were observed. To test whether RAGE was involved in S- to R-phenotypic changes, RAGE was downregulated by using two specific siRNAs. Both RAGE siRNAs markedly decreased RAGE mRNA expression 48 h after transfection compared with the scramble siRNA (50.23 ± 5.78%, $P < 0.01$). The transfection efficiency of S-SMCs, evaluated by transfecting cells with Block-it Fluorescent Oligo for 48 h, represented more than 90% (data not shown). In the presence of extracellular S100A4-rich CM for 1 h, translocation of NF-κB from the cytosol to the nucleus was entirely abolished after transfection of both RAGE-specific siRNAs compared with scramble siRNA (Fig. 9C). Recently, it has been shown that inhibition of RAGE by using a RAGE antagonistic peptide (RAP) prevented the interaction between RAGE and S100A4 [25]. Pre-treatment of S-SMCs with RAP for 30 min abolished NF-κB translocation and decreased significantly BrdU incorporation induced by extracellular S100A4-rich CM (14.5 ± 0.50% vs 17.3 ± 0.25%, $P < 0.05$). Furthermore, pre-treatment of S-SMCs with PDTC (inhibitor of NF-κB) inhibited NF-κB translocation (Fig. 9B). In these conditions (RAGE siRNAs, RAP treatment and PDTC pre-treatment), the S- to R-phenotypic changes induced by extracellular S100A4-rich CM were prevented only in approximately 50% of cells (Fig. 9E, a and d). This was accompanied by a downregulation of S100A4 (Fig. 9E, b and e) and an upregulation of α-SMA (Fig. 9E, c and f). Our results indicate that extracellular S100A4 acts on SMC phenotype at least partly in a RAGE-dependent manner.

4. Discussion

In the present study we demonstrate that the extracellular form of S100A4, marker of R-SMCs in vitro and intimal SMCs in vivo, is a key modulator of SMC phenotypic transition. By transfecting a human S100A4-containing plasmid in S-SMCs (nearly devoid of S100A4), we showed that the S100A4-overexpressing SMCs released high levels of S100A4 into the cell supernatant, inducing a S- to R-phenotypic change

Table 3
Expression of MMP and TIMP mRNAs in S100A4-rich CM treated S-SMCs and native R-SMCs compared to their respective controls.

	S-SMCs treated with			Native		
	pcDNA3-CM	S100A4-CM	*P*	S-SMC	R-SMCs	*P*
MMP-1	1.61 ± 0.001	28.64 ± 0.03	$P < 0.001$	8.25 ± 0.02	0.82 ± 0.01	$P < 0.05$
MMP-2	68.85 ± 0.09	126.37 ± 0.03	$P < 0.01$	78.29 ± 0.06	105.63 ± 0.11	$P < 0.05$
MMP-3	2.87 ± 0.01	69.56 ± 0.08	$P < 0.001$	5.54 ± 0.02	0.31 ± 0.00	$P < 0.05$
MMP-9	18.11 ± 0.06	69.14 ± 0.13	$P < 0.01$	38.83 ± 0.12	37.45 ± 0.13	NS
MMP-14	117.30 ± 0.11	74.42 ± 0.03	$P < 0.001$	106.19 ± 0.19	93.27 ± 0.14	NS
uPA	64.91 ± 0.03	92.42 ± 0.07	$P < 0.05$	87.92 ± 0.11	121.24 ± 0.12	$P < 0.05$
TIMP-1	37.75 ± 0.01	102.44 ± 0.08	$P < 0.01$	62.14 ± 0.15	19.74 ± 0.04	$P < 0.05$
TIMP-3	2.09 ± 0.001	0.74 ± 0.01	$P < 0.01$	5.34 ± 0.01	80.24 ± 0.22	$P < 0.01$

mRNA expression is normalized to GAPDH mRNA expression (%).

of the whole SMC population; this S100A4-rich CM, when added to S-SMCs, induced a rapid transition from the S- to R-phenotype. Conversely, blockade of extracellular S100A4, released by native R-SMCs using a specific neutralizing antibody, reversed the phenotype from R to S. Besides, silencing of S100A4 in R-SMCs, which does not modify the level of extracellular S100A4, had no effect on the SMC phenotype, indicating that the extracellular S100A4 is responsible for the persistence of the R-phenotype.

SMC phenotypic transition towards a R-phenotype, induced by extracellular S100A4, was associated with an early increase in cell

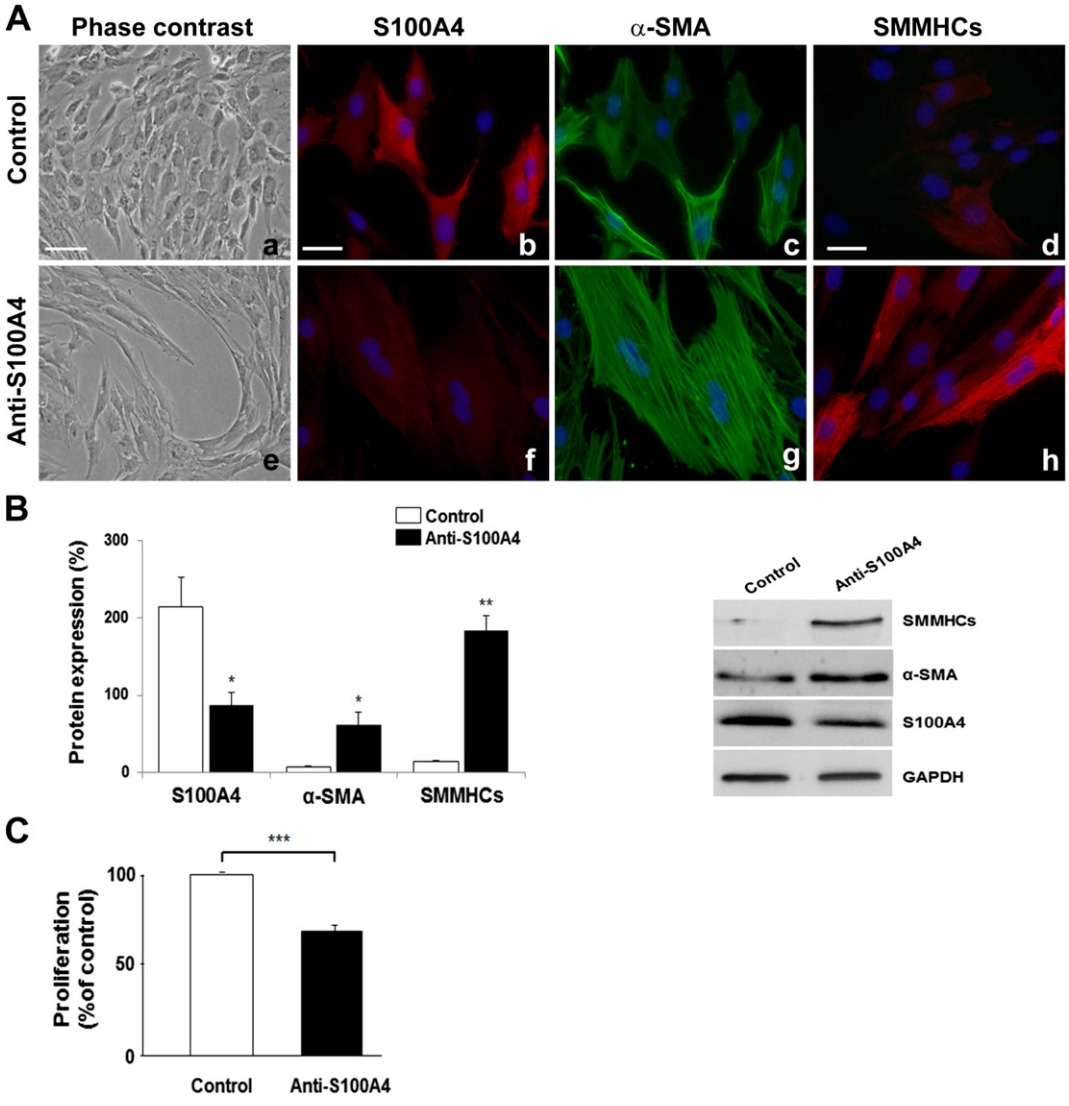

Fig. 6. Effect of extracellular S100A4 neutralization on R-SMC phenotype. A, Phase-contrast photomicrographs (a and e) and double immunofluorescence staining showing S100A4 (b and f), α-SMA (c and g) and SMMHC (d and h) expression in R-SMCs treated for 96 h with unspecific rabbit polyclonal (a–d) or S100A4 neutralizing (e–h) antibodies (n = 4). In (a and e), bar = 75 μm; in (b, c, f and g), bar = 25 μm; in (d and h), bar = 10 μm. B, Bar graphs and representative immunoblots showing S100A4, α-SMA, and SMMHC expression normalized to GAPDH content in R-SMCs treated for 96 h with unspecific rabbit polyclonal or S100A4 neutralizing antibodies (n = 3). C, Bar graph showing proliferation of R-SMCs treated for 96 h with unspecific rabbit polyclonal (control, open bar) or S100A4 neutralizing (anti-S100A4, filled bar) antibodies (n = 4).

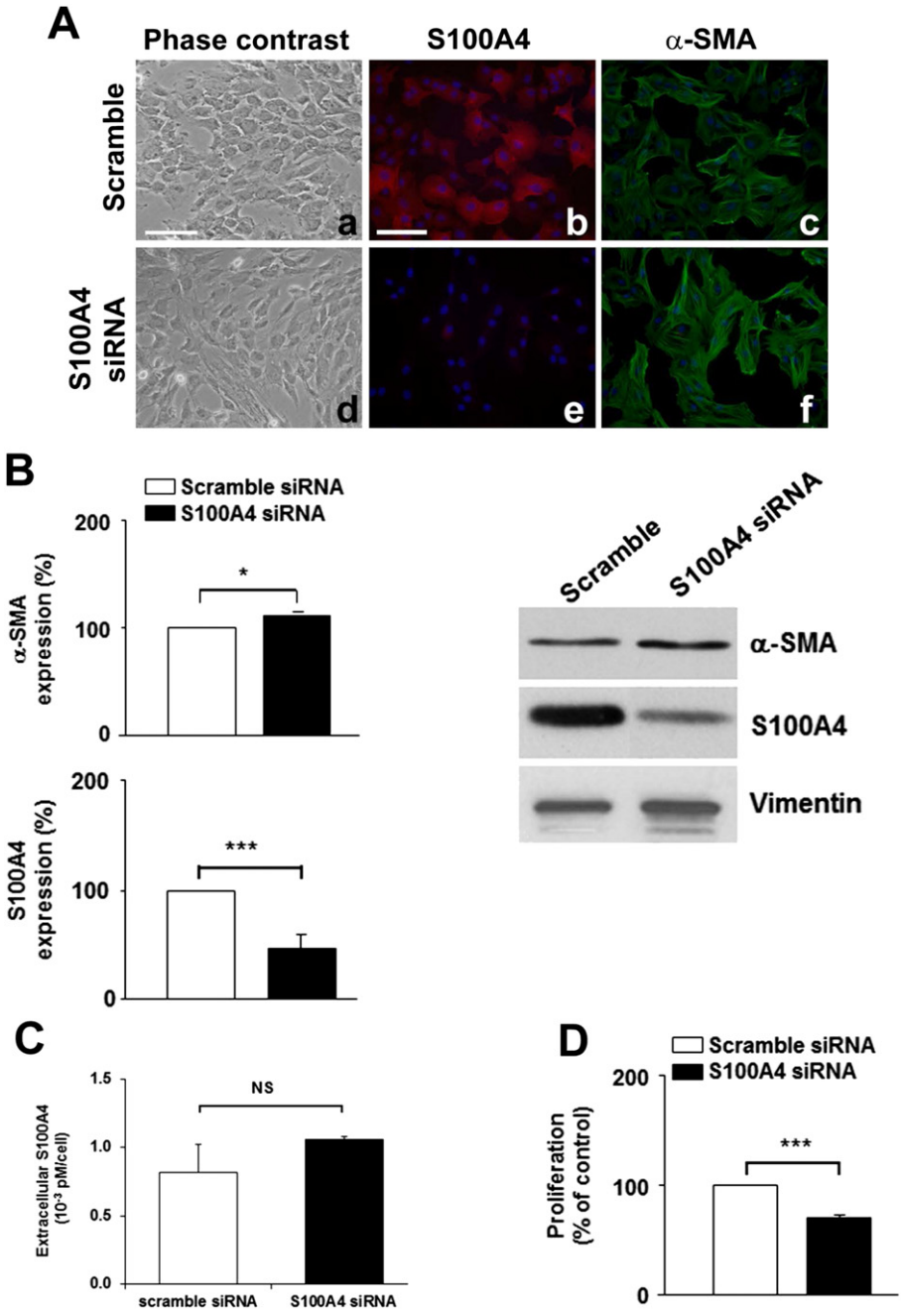

Fig. 7. Effect of endogenous S100A4 downregulation on the R-SMC phenotype. A, Phase-contrast photomicrographs (a and d) and double immunofluorescence staining showing S100A4 (b and e) and α-SMA (c and f) expression in R-SMCs 48 h after transfection with scramble (a–c) and S100A4 (e–h) siRNA (n = 6). Nuclei are stained in blue by DAPI. In (a and d), bar = 75 μm; in (b, c, e and f), bar = 25 μm. B, Bar graph and representative immunoblots showing S100A4 and α-SMA expression normalized to vimentin content in R-SMCs 48 h after transfection with scramble (open bars) and S100A4 (filled bars) siRNA. C, Bar graph showing extracellular S100A4 content detected by competitive ELISA in R-SMC supernatants after transfection with scramble (open bars) and S100A4 (filled bars) siRNA (n = 4). D, Bar graph showing cell proliferation in R-SMCs 48 h after transfection with scramble (open bars) and S100A4 (filled bars) siRNA. *** = $P < 0.001$; ** = $P < 0.01$, * = $P < 0.05$; NS, not significant.

migration and later to a marked increase in cell proliferation, upregulation of intracellular S100A4 as well as downregulation of SMC differentiation markers (α-SMA, SMMHCs, SM22-α and smoothelin). In addition, PDGF-BB and c-myc were upregulated. The reverse processes were observed when the extracellular S100A4 was neutralized with a specific antibody. Likewise, neutralization of extracellular S100A4 activity with rabbit polyclonal S100A4 antibody has been shown to attenuate pulmonary artery SMC migration [19]. Our results also suggest that intracellular S100A4 and SMC differentiation marker expression changes likely result from the cell morphological transition. Nonetheless extracellular S100A4 has been shown to induce endogenous protein translocation of intracellular S100A4 in endothelial cells [12]. However, there is no direct evidence that extracellular S100A4 is a potent regulator of intracellular S100A4.

S100A4 is recognized as a mediator of cancer metastasis [8]. It exhibits both extracellular and intracellular functions [6,26]. S100 proteins exhibit distinct translocation pathways within cells [12,27] but their mechanisms of secretion are still obscure. The extracellular activity of S100A4 is associated with the dimeric and the oligomeric conformation of the protein. It has been detected both in vitro, in the CM of cancer cell lines and of human pulmonary artery SMCs under sustained hypoxia [19], and in vivo, in serum of patients with cancer and rheumatoid arthritis [9]. The role of extracellular S100A4 in the metastatic process has been demonstrated by adding recombinant S100A4 in culture

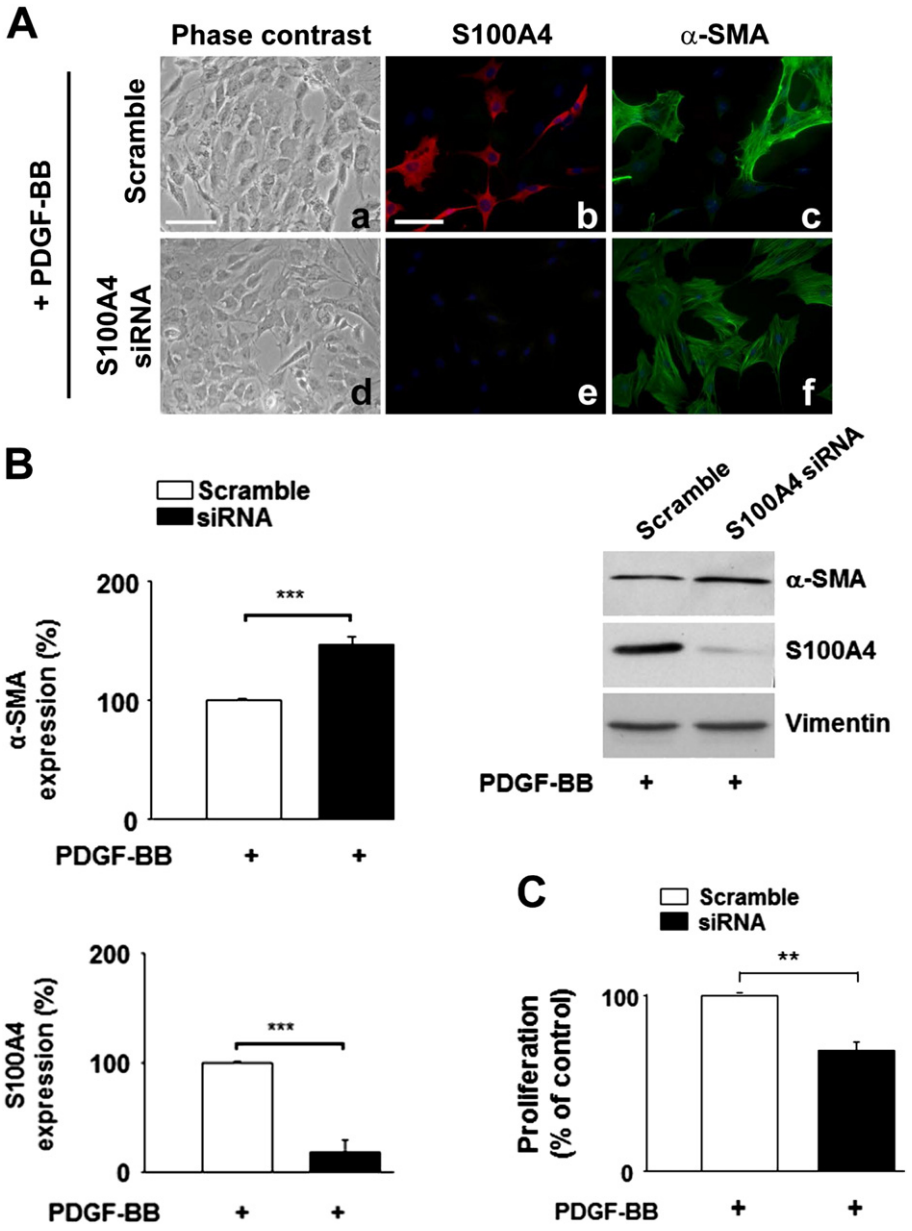

Fig. 8. Effect of intracellular S100A4 downregulation on PDGF-BB-induced S- to R-phenotype. A, Phase-contrast photomicrographs (a and d) and double immunofluorescence staining showing S100A4 (b and e) and α-SMA (c and f) expression in S-SMCs 48 h after transfection with scramble (a–c) and S100A4 (d–f) siRNA in the presence of PDGF-BB (30 ng/mL, n = 4). Nuclei are stained in blue by DAPI. In (a and d), bar = 75 μm; in (b, c, e and f), bar = 25 μm. B, Bar graph and representative immunoblots showing S100A4 and α-SMA expression normalized to vimentin content in S-SMCs 48 h after transfection with scramble (open bars) and S100A4 (filled bars) siRNA in the presence of PDGF-BB (30 ng/mL, n = 3). C, Bar graph showing cell proliferation in S-SMCs 48 h after transfection with scramble (open bars) and S100A4 (filled bars) siRNA in the presence of PDGF-BB (30 ng/mL, n = 3). *** = $P < 0.001$; ** = $P < 0.01$.

medium of several target cells: recombinant S100A4 stimulates the metastatic potential of S100A4-negative mouse mammary carcinoma cells [28], and the angiogenesis of endothelial cells [29]. Moreover extracellular S100A4 activity is correlated with extracellular matrix remodeling (i.e. increased production of MMP-13 by endothelial cells [28]). In our model, we observed that treatment of S-SMCs with commercially available recombinant S100A4 failed to act on SMC phenotypic changes (data not shown), suggesting that the dimeric or oligomeric conformation of the protein may be important for its activity [6,30]. Nevertheless treatment of S-SMCs with S100A4-rich CM as a source of extracellular S100A4 and blockade of extracellular S100A4 in R-SMCs with a specific neutralizing antibody clearly established the role of extracellular S100A4 in SMC phenotypic transition.

Several studies demonstrate that extracellular S100A4 activates NF-κB in several cell types [11,28,31]. These signaling events can be dependent or independent on RAGE resulting in increased production of MMPs [11,12,28]. Extracellular S100A4 could also act on rat neuritogenesis through heparin sulfate proteoglycan [32] and plasmin formation through interaction with annexin II [29]. In atherosclerotic plaque progression, RAGE is upregulated as a cellular response to pathogenic environment. In diabetic mice, RAGE is upregulated at sites of accelerated vascular lesions and its inhibition reduces these lesions [33]. Likewise, RAGE blockade lowers SMC proliferation and neointimal formation after balloon-injury in mice [33]. It contributes to intimal thickening development by promoting inflammation, cell migration and proliferation, and oxidative stress [33–35]. In humans, expression of RAGE is significantly greater in the atheromatous plaque of diabetic patients and is associated with SMC and macrophage apoptosis [36], suggesting that RAGE promotes plaque destabilization. Rabinovitch and collaborators have observed that extracellular S100A4 leads to

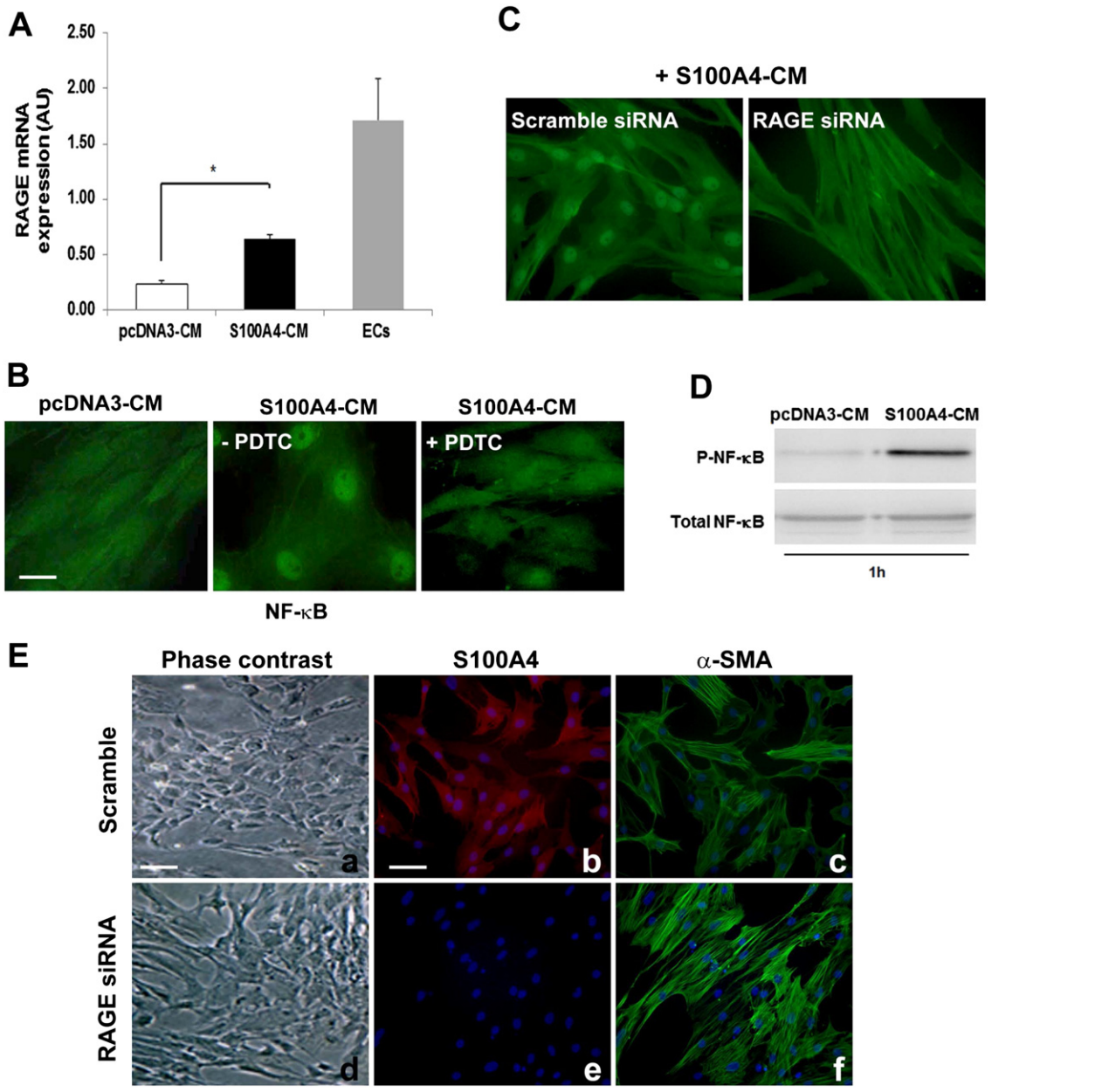

Fig. 9. Effect of extracellular S100A4-rich CM on RAGE and NF-κB activation. A, Bar graph showing RAGE mRNA quantification by real-time PCR normalized to GAPDH mRNA expression in S-SMCs treated for 4 h with CM collected from pcDNA3 (open bar) or pcDNA3-S100A4 (filled bar) vector transfected S-SMCs (48 h post-transfection, n = 4). Endothelial cells were used as a positive control. B, Immunofluorescence staining showing NF-κB expression in S-SMCs treated for 1 h with CM collected from pcDNA3 or pcDNA3-S100A4 vector transfected S-SMCs pre-treated with PDTC or not for 30 min (n = 3), bar = 25 μm. C, Immunofluorescence staining showing NF-κB expression in S-SMCs 48 h after transfection of scramble or RAGE siRNA treated for 1 h with CM collected from pcDNA3-S100A4 vector transfected S-SMCs (n = 3), bar = 10 μm. D, Representative immunoblots showing phosphorylated NF-κB (P-NF-κB) and total NF-κB expression in S-SMCs treated for 1 h with CM collected from pcDNA3 or pcDNA3-S100A4 vector transfected S-SMCs (n = 3). E, Phase-contrast photomicrographs (a and d) and immunofluorescence staining showing S100A4 (b and e) and α-SMA (c and f) expression in S-SMCs 48 h after transfection with scramble (a–c) or RAGE siRNA (d–f, n = 6). Nuclei are stained in blue by DAPI. In (a and d), bar = 75 μm; in (b, c, e and g), bar = 10 μm. *** = $P < 0.001$; NS, not significant; AU, arbitrary units.

human pulmonary artery SMC proliferation and migration in a RAGE-dependent manner [31]. They have further reported that extracellular S100A4 and bone morphogenic protein-4 (BMP-4) can recruit multiple cell surface receptors, i.e. RAGE and BMP receptor II, to induce cell motility [37]. S100A4 could also interact with other receptors such as Toll-like receptors [38,39]. The situation is even more complex in that S100 proteins exist in different forms (dimers, tetramers, higher oligomers) interacting with RAGE, which itself does not float as a molecule in the plasma membrane but instead agglomerates into receptor assemblies [7,39,40]. Here we showed that RAGE downregulation using silencing siRNA or a specific RAGE antagonistic peptide [25] decreased cell proliferation and only partially prevented the S- to R-phenotypic change induced by S100A4-rich CM even if NF-κB activation was fully abolished. Therefore, a co-dependence between RAGE and not yet identified receptor(s) could mediate extracellular S100A4-induced porcine arterial SMC phenotypic transition.

We demonstrated that native R-SMCs expressed and released S100A4. Unexpectedly, silencing of S100A4 mRNA did not change the level of extracellular S100A4 in the supernatant or SMC morphology in spite of decreased proliferative activity and increased level of differentiation (i.e. increased α-SMA expression). These results confirm that the extracellular S100A4 is responsible for the persistence of the R-phenotype.

We demonstrated that treatment of S-SMCs with PDGF-BB enhanced SMC proliferation and promoted a switch towards the R-phenotype [3], which was associated with S100A4 upregulation [4].

PDGF-BB is known to induce rather profound suppression of SMC differentiation markers and increase SMC proliferation [23]. We further showed that silencing of S100A4 mRNA did not prevent the S- to R-phenotypic transition induced by PDGF-BB treatment. However, SMC proliferation was decreased and α-SMA expression was significantly increased. These results indicate that intracellular S100A4 affects essentially SMC proliferation. Intracellular S100A4 acts on target proteins such as p53 [13], non-muscle MHC [16], actin [17] and non-muscle tropomyosin [18]. Such interactions could explain the role of intracellular S100A4 in SMC proliferation and migration. Therefore extracellular S100A4 and intracellular S100A4 play distinct roles on SMC phenotypic changes.

To ascertain that extracellular S100A4-rich CM treatment yielded a R-phenotype identical to the one of native R-SMCs, we assessed several genes typically involved in SMC phenotypic transition. The profile of gene expression typical of the synthetic phenotype (i.e. the native R-SMCs isolated from the porcine coronary artery) such as differentiation/dedifferentiation markers [3,4], MMP-2 and uPA [3,41], was similar in both situations. Unexpectedly, the profile of proteolytic enzymes and inhibitors was different in both situations. In particular, MMP-1, -3 and -9, promoting plaque instability [41] were increased in S100A4-rich CM treated S-SMCs compared with native R-SMCs whereas TIMP-3 related to plaque stability [42] was decreased. Our results suggest that S100A4-rich CM treated S-SMCs exhibit a profile of activated SMCs [43] i.e. a proinflammatory signature that could be involved in the extracellular matrix remodeling leading to plaque vulnerability.

5. Conclusion

We show that extracellular S100A4 is essential for the establishment of the synthetic phenotype in porcine coronary artery, shedding light on the mechanisms of SMC accumulation in the intima. Interestingly, extracellular S100A4 mostly recapitulates the mRNA profile observed in native R-SMCs but might in addition promote a deleterious SMC phenotype. This finding related to our previous observation that S100A4 is an in vivo marker of intimal SMCs in human indicates that extracellular S100A4 could be a new target to prevent the evolution of atherosclerosis and restenosis. Further studies exploring receptors, signaling pathways and target genes activated by extracellular S100A4 will be useful to better understand these pathological processes.

Acknowledgements

We are particularly grateful to Christine Chaponnier for her invaluable technical advice, discussions and suggestions. We thank Aman Ahmed-Mohamed for her excellent technical assistance.

Sources of funding

This study was supported by the Swiss National Science Foundation grant # 146790/1, the Foundations Simone et Gustave Prévot, Artères, Reuters (Geneva, Switzerland), and Swiss Life (Zürich, Switzerland).

References

[1] K.R. Stenmark, K.A. Fagan, M.G. Frid, Hypoxia-induced pulmonary vascular remodeling: cellular and molecular mechanisms, Circ. Res. 99 (2006) 675–691.
[2] C. Chaabane, F. Otsuka, R. Virmani, M.L. Bochaton-Piallat, Biological responses in stented arteries, Cardiovasc. Res. 99 (2013) 353–363.
[3] H. Hao, P. Ropraz, V. Verin, E. Camenzind, A. Geinoz, M.S. Pepper, G. Gabbiani, M.L. Bochaton-Piallat, Heterogeneity of smooth muscle cell populations cultured from pig coronary artery, Arterioscler. Thromb. Vasc. Biol. 22 (2002) 1093–1099.
[4] A.C. Brisset, H. Hao, E. Camenzind, M. Bacchetta, A. Geinoz, J.C. Sanchez, C. Chaponnier, G. Gabbiani, M.L. Bochaton-Piallat, Intimal smooth muscle cells of porcine and human coronary artery express S100A4, a marker of the rhomboid phenotype in vitro, Circ. Res. 100 (2007) 1055–1062.
[5] M. Coen, G. Marchetti, P.M. Palagi, C. Zerbinati, G. Guastella, T. Gagliano, F. Bernardi, F. Mascoli, M.L. Bochaton-Piallat, Calmodulin expression distinguishes the smooth muscle cell population of human carotid plaque, Am. J. Pathol. 183 (2013) 996–1009.
[6] E. Leclerc, C.W. Heizmann, The importance of Ca^{2+}/Zn^{2+} signaling S100 proteins and RAGE in translational medicine, Front. Biosci. (Schol. Ed.) 3 (2011) 1232–1262.
[7] S.R. Gross, C.G. Sin, R. Barraclough, P.S. Rudland, Joining S100 proteins and migration: for better or for worse, in sickness and in health, Cell. Mol. Life Sci. 71 (2014) 1551–1579.
[8] G.V. Sherbet, Metastasis promoter S100A4 is a potentially valuable molecular target for cancer therapy, Cancer Lett. 280 (2009) 15–30.
[9] M. Grigorian, N. Ambartsumian, E. Lukanidin, Metastasis-inducing S100A4 protein: implication in non-malignant human pathologies, Curr. Mol. Med. 8 (2008) 492–496.
[10] M. Dahlmann, A. Okhrimenko, P. Marcinkowski, M. Osterland, P. Herrmann, J. Smith, C.W. Heizmann, P.M. Schlag, U. Stein, RAGE mediates S100A4-induced cell motility via MAPK/ERK and hypoxia signaling and is a prognostic biomarker for human colorectal cancer metastasis, Oncotarget 5 (2014) 3220–3233.
[11] R.R. Yammani, D. Long, R.F. Loeser, Interleukin-7 stimulates secretion of S100A4 by activating the JAK/STAT signaling pathway in human articular chondrocytes, Arthritis Rheum. 60 (2009) 792–800.
[12] H.L. Hsieh, B.W. Schafer, B. Weigle, C.W. Heizmann, S100 protein translocation in response to extracellular S100 is mediated by receptor for advanced glycation endproducts in human endothelial cells, Biochem. Biophys. Res. Commun. 316 (2004) 949–959.
[13] M.R. Fernandez-Fernandez, D.B. Veprintsev, A.R. Fersht, Proteins of the S100 family regulate the oligomerization of p53 tumor suppressor, Proc. Natl. Acad. Sci. U. S. A. 102 (2005) 4735–4740.
[14] E. Lukanidin, J.P. Sleeman, Building the niche: the role of the S100 proteins in metastatic growth, Semin. Cancer Biol. 22 (2012) 216–225.
[15] J. Klingelhofer, H.D. Moller, E.U. Sumer, C.H. Berg, M. Poulsen, D. Kiryushko, V. Soroka, N. Ambartsumian, M. Grigorian, E.M. Lukanidin, Epidermal growth factor receptor ligands as new extracellular targets for the metastasis-promoting S100A4 protein, FEBS J. 276 (2009) 5936–5948.
[16] E.J. Kim, D.M. Helfman, Characterization of the metastasis-associated protein, S100A4. Roles of calcium binding and dimerization in cellular localization and interaction with myosin, J. Biol. Chem. 278 (2003) 30063–30073.
[17] A. Mandinova, D. Atar, B.W. Schafer, M. Spiess, U. Aebi, C.W. Heizmann, Distinct subcellular localization of calcium binding S100 proteins in human smooth muscle cells and their relocation in response to rises in intracellular calcium, J. Cell Sci. 111 (Pt 14) (1998) 2043–2054.
[18] K. Takenaga, Y. Nakamura, S. Sakiyama, Y. Hasegawa, K. Sato, H. Endo, Binding of pEL98 protein, an S100-related calcium-binding protein, to nonmuscle tropomyosin, J. Cell Biol. 124 (1994) 757–768.
[19] M.G. Frid, M. Li, M. Gnanasekharan, D.L. Burke, M. Fragoso, D. Strassheim, J.L. Sylman, K.R. Stenmark, Sustained hypoxia leads to the emergence of cells with enhanced growth, migratory, and promitogenic potentials within the distal pulmonary artery wall, Am. J. Physiol. Lung Cell. Mol. Physiol. 297 (2009) L1059–L1072.
[20] O. Skalli, P. Ropraz, A. Trzeciak, G. Benzonana, D. Gillessen, G. Gabbiani, A monoclonal antibody against alpha-smooth muscle actin: a new probe for smooth muscle differentiation, J. Cell Biol. 103 (1986) 2787–2796.
[21] G.A. Stouffer, G.K. Owens, Angiotensin II-induced mitogenesis of spontaneously hypertensive rat-derived cultured smooth muscle cells is dependent on autocrine production of transforming growth factor-b, Circ. Res. 70 (1992) 820–828.
[22] M.M. Bradford, A rapid and sensitive method for the quantification of microgram quantities of protein utilizing the principle of protein-dye binding, Anal. Biochem. 72 (1976) 248–254.
[23] T. Yoshida, G.K. Owens, Molecular determinants of vascular smooth muscle cell diversity, Circ. Res. 96 (2005) 280–291.
[24] E. Leclerc, Measuring binding of S100 proteins to RAGE by surface plasmon resonance, Methods Mol. Biol. 963 (2013) 201–213.
[25] T. Arumugam, V. Ramachandran, S.B. Gomez, A.M. Schmidt, C.D. Logsdon, S100P-derived RAGE antagonistic peptide reduces tumor growth and metastasis, Clin. Cancer Res. 18 (2012) 4356–4364.
[26] R. Donato, Intracellular and extracellular roles of S100 proteins, Microsc. Res. Tech. 60 (2003) 540–551.
[27] H.L. Hsieh, B.W. Schafer, J.A. Cox, C.W. Heizmann, S100A13 and S100A6 exhibit distinct translocation pathways in endothelial cells, J. Cell Sci. 115 (2002) 3149–3158.
[28] B. Schmidt-Hansen, D. Ornas, M. Grigorian, J. Klingelhofer, E. Tulchinsky, E. Lukanidin, N. Ambartsumian, Extracellular S100A4(mts1) stimulates invasive growth of mouse endothelial cells and modulates MMP-13 matrix metalloproteinase activity, Oncogene 23 (2004) 5487–5495.
[29] A. Semov, M.J. Moreno, A. Onichtchenko, A. Abulrob, M. Ball, I. Ekiel, G. Pietrzynski, D. Stanimirovic, V. Alakhov, Metastasis-associated protein S100A4 induces angiogenesis through interaction with annexin II and accelerated plasmin formation, J. Biol. Chem. 280 (2005) 20833–20841.
[30] S.B. Carvalho, H.M. Botelho, S.S. Leal, I. Cardoso, G. Fritz, C.M. Gomes, Intrinsically disordered and aggregation prone regions underlie beta-aggregation in S100 proteins, PLoS One 8 (2013) e76629.
[31] A. Lawrie, E. Spiekerkoetter, E.C. Martinez, N. Ambartsumian, W.J. Sheward, M.R. MacLean, A.J. Harmar, A.M. Schmidt, E. Lukanidin, M. Rabinovitch, Interdependent serotonin transporter and receptor pathways regulate S100A4/Mts1, a gene associated with pulmonary vascular disease, Circ. Res. 97 (2005) 227–235.
[32] D. Kiryushko, V. Novitskaya, V. Soroka, J. Klingelhofer, E. Lukanidin, V. Berezin, E. Bock, Molecular mechanisms of Ca(2+) signaling in neurons induced by the S100A4 protein, Mol. Cell. Biol. 26 (2006) 3625–3638.

[33] Y. Naka, L.G. Bucciarelli, T. Wendt, L.K. Lee, L.L. Rong, R. Ramasamy, S.F. Yan, A.M. Schmidt, RAGE axis: animal models and novel insights into the vascular complications of diabetes, Arterioscler. Thromb. Vasc. Biol. 24 (2004) 1342–1349.
[34] J.L. Wautier, A.M. Schmidt, Protein glycation: a firm link to endothelial cell dysfunction, Circ. Res. 95 (2004) 233–238.
[35] A. Bierhaus, P.M. Humpert, M. Morcos, T. Wendt, T. Chavakis, B. Arnold, D.M. Stern, P.P. Nawroth, Understanding RAGE, the receptor for advanced glycation end products, J. Mol. Med. (Berl.) 83 (2005) 876–886.
[36] A.P. Burke, F.D. Kolodgie, A. Zieske, D.R. Fowler, D.K. Weber, P.J. Varghese, A. Farb, R. Virmani, Morphologic findings of coronary atherosclerotic plaques in diabetics: a postmortem study, Arterioscler. Thromb. Vasc. Biol. 24 (2004) 1266–1271.
[37] E. Spiekerkoetter, C. Guignabert, V. de Jesus Perez, T.P. Alastalo, J.M. Powers, L. Wang, A. Lawrie, N. Ambartsumian, A.M. Schmidt, M. Berryman, R.H. Ashley, M. Rabinovitch, S100A4 and bone morphogenetic protein-2 codependently induce vascular smooth muscle cell migration via phospho-extracellular signal-regulated kinase and chloride intracellular channel 4, Circ. Res. 105 (2009) 639–647.
[38] L.A. Cerezo, M. Remakova, M. Tomcik, S. Gay, M. Neidhart, E. Lukanidin, K. Pavelka, M. Grigorian, J. Vencovsky, L. Senolt, The metastasis-associated protein S100A4 promotes the inflammatory response of mononuclear cells via the TLR4 signalling pathway in rheumatoid arthritis, Rheumatology (Oxford) 53 (2014) 1520–1526.
[39] Z.A. Ibrahim, C.L. Armour, S. Phipps, M.B. Sukkar, RAGE and TLRs: relatives, friends or neighbours? Mol. Immunol. 56 (2013) 739–744.
[40] A. Rouhiainen, J. Kuja-Panula, S. Tumova, H. Rauvala, RAGE-mediated cell signaling, Methods Mol. Biol. 963 (2013) 239–263.
[41] A.C. Newby, Matrix metalloproteinase inhibition therapy for vascular diseases, Vasc. Pharmacol. 56 (2012) 232–244.
[42] W.C. Huang, G.B. Sala-Newby, A. Susana, J.L. Johnson, A.C. Newby, Classical macrophage activation up-regulates several matrix metalloproteinases through mitogen activated protein kinases and nuclear factor-kappaB, PLoS One 7 (2012) e42507.
[43] D. Gomez, G.K. Owens, Smooth muscle cell phenotypic switching in atherosclerosis, Cardiovasc. Res. 95 (2012) 156–164.